Protein Science (1998), 7:886–896. Cambridge University Press. Printed in the USA.

LIF receptor–gp130 interaction investigated by homology modeling: Implications for LIF binding

DAVID K. SMITH[1,2,3] AND HERBERT R. TREUTLEIN[1]

[1]Molecular Modelling Group, Ludwig Institute for Cancer Research, and Cooperative Research Centre for Cellular Growth Factors, Royal Melbourne Hospital, Parkville, Victoria, 3050, Australia
[2]Biochemistry Department, University of Melbourne, Parkville, Victoria, 3052, Australia

(RECEIVED July 23, 1997; ACCEPTED December 20, 1997)

Abstract

Leukemia inhibitory factor (LIF), a member of the gp130 family of helical cytokines, is involved in the hemopoietic and neural systems. The LIF signal transducing complex contains two receptor molecules, the LIF receptor (LIFR) and gp130. The extracellular region of the LIFR is unique in that it includes three membrane-proximal fibronectin type III domains and two cytokine binding domains (CBDs) separated by an immunoglobulin-like domain. Although some mutagenesis data on LIF are available, it is not yet known which regions of LIFR or gp130 bind LIF. Nor is it known whether LIFR contacts gp130 in a manner similar to the growth hormone receptor dimer and, if so, through which of its CBDs. To attempt to elucidate these matters and to investigate the receptor complex, models of the CBDs of LIFR and the CBD of gp130 were constructed. Analyses of the electrostatic isopotential surfaces of the CBD models suggest that gp130 and the membrane-proximal CBD of LIFR hetero-dimerize and bind LIF through contacts similar to those seen in the growth hormone receptor dimer. This work further demonstrates the utility of electrostatic analyses of homology models and suggests a strategy for biochemical investigations of the LIF–receptor complex.

Keywords: cytokine receptor; electrostatics; homology modeling; LIF

Leukemia inhibitory factor is a pleiotropic helical cytokine that acts on a wide range of cell types in the hemopoietic and neural systems (Bazan, 1991; Hilton, 1992; Metcalf, 1992; Patterson, 1994). It is a member of the cytokine family that signals via gp130: interleukin-6, IL-11, oncostatin M, ciliary neurotrophic factor, and cardiotrophin-1 (Kishimoto et al., 1995). The sharing of gp130 as a component of the receptor complexes of these cytokines is believed to explain the redundancy of function seen among the group (Kishimoto et al., 1995). For example, it has been shown that LIF is not essential for survival in mice, its functions apparently replaced by other members of the gp130 family, because LIF-deficient mice are viable (Stewart et al., 1992). LIF does not seem to play a role in neural development, but is involved in responses to nerve injury (Rao et al., 1993; Cheema et al., 1994; Patterson, 1994; Tham et al., 1997) and may thereby have an important therapeutic role in neurodegenerative disorders. However, the LIF receptor has been shown to be essential for survival in mice (Li et al., 1995; Ware et al., 1995).

Receptors for the helical cytokines form a family of membrane-bound molecules whose extracellular domains are highly modular, consisting of fibronectin type III and immunoglobulin-like domains (Cosman, 1993; Sprang & Bazan, 1993). Two conserved disulfide bridges in one FnIII domain and a conserved sequence motif ("WSXWS") in the adjoining FnIII domain first identified the family called the class I cytokine receptors (Bazan, 1990). These tandem FnIII domains form the cytokine-binding domain, which is the only component of the extracellular domain of many helical cytokine receptors, such as the growth hormone, prolactin, and erythropoietin receptors (Cosman, 1993). Other cytokine receptors also have extracellular domains containing a CBD adjacent to the membrane with an N-terminal Ig-like domain (e.g., IL-6R, CNTFR) or a second CBD (e.g., the common β-chain). Another group of receptors has three FnIII domains adjacent to the membrane and an N-terminal region that consists of either a CBD (e.g., IL-12R), a CBD and an Ig-like domain (e.g., gp130), two CBDs separated by an Ig-like domain (LIFR) and the OSM receptor, which is like LIFR, but lacks the N-terminal FnIII domain of the N-terminal CBD (Cosman, 1993; Chua et al., 1994; Mosley et al., 1996). The receptors for the interferons and IL-10, along with tissue factor, form a related group known as the class II cytokine receptors (Bazan, 1990).

Reprint requests to: H.R. Treutlein, Molecular Modelling Group, Ludwig Institute for Cancer Research, PO Box 2008, Royal Melbourne Hospital, Parkville, Victoria, 3050, Australia; e-mail: treutlei@ludwig.edu.au.
[3]Present address: Biochemistry Department, Hong Kong University of Science and Technology, Clear Water Bay, Kowloon, Hong Kong.

Abbreviations: LIF, leukemia inhibitory factor; GH, growth hormone; IL, interleukin; CNTF, ciliary neurotrophic factor; OSM, oncostatin M; CT-1, cardiotrophin; G-CSF, granulocyte colony-stimulating factor; R, (after cytokine name) the specific receptor for that cytokine; CBD, cytokine binding domain; FnIII, fibronectin type III; first CBD, the N-terminal CBD; second CBD, the membrane-proximal CBD; Ig, immunoglobulin.

To date, only one complete helical cytokine and receptor complex, that of growth hormone and its receptors, has had its three-dimensional structure determined (de Vos et al., 1992; Sundström et al., 1996). Partial complexes are known for a 1:1 growth hormone–growth hormone receptor complex (Sundström et al., 1996), GH and the prolactin receptor (Somers et al., 1994), two erythropoietin receptors with a synthetic ligand (Livnah et al., 1996), and interferon γ and its receptor α-chain (Walter et al., 1995). Also, the structure of the related class II cytokine receptor molecule, tissue factor, has been determined in the free (Harlos et al., 1994; Muller et al., 1994, 1996) and ligand-bound (Banner et al., 1996) forms. The complex of growth hormone and its receptors has formed the paradigm for helical cytokine binding. One receptor binds the cytokine at site I (consisting of the exposed faces of the D and A helices) and then the second receptor binds to site II (the A and C helices) assisted by binding to a region on the other receptor (de Vos et al., 1992; Wells, 1996; Wells & de Vos, 1996). This two-site binding pattern, sometimes with a third site, appears to be a common motif in helical cytokine–receptor interactions (Mott & Campbell, 1995; Paonessa et al., 1995).

Extensive mutagenesis studies have been performed on the growth hormone complex (Cunningham et al., 1991; Cunningham & Wells, 1993; Clackson & Wells, 1995) showing that the structurally defined binding epitope is much larger than the functionally defined epitope (de Vos et al., 1992; Cunningham & Wells, 1993; Clackson & Wells, 1995). Hydrophobic interactions are important in the ligand–receptor interaction (Clackson & Wells, 1995), but electrostatic interactions are also important in growth hormone binding (Cunningham & Wells, 1993). Calculations of electrostatic potential surfaces of the receptors and the ligand have shown that they are clearly complementary (Demchuk et al., 1994) with growth hormone, having a symmetric electrostatic potential surface, consistent with it binding two identical receptors. When the asymmetry of the dimer interface between the two growth hormone receptors is taken into account, it can be seen that the receptors also show a clear electrostatic complementarity in the dimer interface region (Smith, 1996; Layton et al., 1997).

Although the crystal structure of LIF has been solved (Robinson et al., 1994), comparatively few data on the interaction of LIF with its receptors are available. LIF has been shown to associate with LIFR at low affinity and then to bind to gp130 to form a high-affinity complex (Gearing et al., 1991, 1992). Competitive binding studies of LIF and CNTF to the common components of their receptor complexes, LIFR and gp130, have been performed (Robledo et al., 1996), suggesting that the components associate differently. Chimeric protein studies have identified a group of six amino acids in LIF that are involved in LIFR binding (Owczarek et al., 1993; Layton et al., 1994b). These residues mostly localize to a region consistent with the third binding site seen in cytokines, such as IL-6, which bind to three receptor molecules (Paonessa et al., 1995; Simpson et al., 1997). More recently, predominately alanine mutations of residues in LIF identified several residues that affected both LIFR and gp130 binding (Hudson et al., 1996) and were consistent with a three-site binding model. However, there is some disagreement between the residues found to be important by Layton et al. (1994b) and by Hudson et al. (1996), perhaps due to the different approaches and species of the molecules used in examining different aspects of receptor interactions. Cross species binding studies on LIF and LIFR revealed an unusual pattern of binding (Layton et al., 1994a). Different behavior was observed for murine and human LIF dissociating from their cognate receptors and both LIF species competed less effectively against the cross species molecule for binding to murine LIFR than would be expected from their individual binding affinities (Layton et al., 1994a). It has been suggested that the results from the cross species binding studies could reflect LIF–receptor interactions that differ from the growth hormone paradigm (Layton et al., 1994a, 1994b). This will be discussed in terms of the models constructed here.

This work uses homology modeling to investigate the interactions of LIF with its receptors. Models of the structures of the CBDs of LIFR and the CBD of gp130 were constructed to try to compare the configuration of the LIF–receptor complex with the growth hormone paradigm for helical cytokine–receptor interactions. The models were examined to predict which receptor regions bind to LIF and whether a contact dimer forms between LIFR and gp130. Because the helical cytokine receptors, as a group, show very little sequence similarity, techniques for evaluating protein structures were used to check the validity of the models and the quality of the sequence alignments used. Electrostatic isopotential surface calculations were utilized to identify potential binding surfaces on the model receptors and on LIF. This also allowed an examination of the utility of this technique in the case when the protein–protein interactions of interest are mainly from loop regions, which are difficult to model by homology-based techniques, particularly when the template structures have low sequence similarity. The modeling provides support for the proposal that the LIF receptor complex is similar to the growth hormone paradigm, binding to regions equivalent to sites I and II and with the receptors forming a contact dimer.

Results

Modeling process

The alignments of the CBD sequences used in the modeling are shown in Figure 1. This alignment also shows the detailed secondary structure of GHR and the β-sheets of GHR and the prolactin receptor, the residues important for the GH–GHR interaction, the residues involved in the "WSXWS" structural motif, and the position of the tyrosine corner. On average, the receptors show 20% sequence identity and 40% similarity with this alignment. In the case of the first and second CBDs of LIFR and the CBD of gp130, the sequence identities to GHR are 13%, 13%, and 21%, respectively, and the sequence similarities are 33%, 31%, and 40%, respectively. This low level of sequence identity made the alignment of some of the β-strands difficult and, in some cases, alternative alignments, where the ends of strands were altered by two residues, were considered. Evaluations of the constructed models with ProsaII (Sippl, 1993) and Profiles3D (Lüthy et al., 1992) were used to assist in choosing between the alignments.

A particular difficulty was encountered with the N-terminal FnIII domain of the first CBD of LIFR. This domain contains the four cysteine residues characteristic of the CBDs, however, there are considerably fewer amino acids between the second and third cysteine residues than in most of the helical cytokine receptors. If the cysteine residues are aligned so that the second disulfide bridge position is conserved between the C′ and E strands, then the loop between the B and C strands must be very short. A further consequence of this alignment is that no tyrosine corner (Hemmingsen et al., 1994) is observed between the E and F strands and an unusually long insertion is required between the F and G strands to bring the alignment back into register for the second FnIII domain.

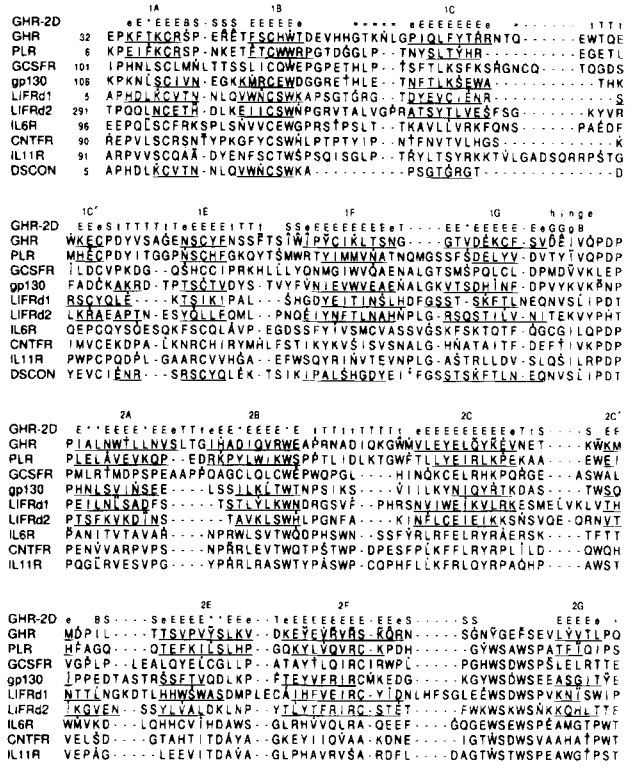

Fig. 1. Alignment of the CBDs of the human gp130 family of receptors and G-CSFR. Numbering is from the mature sequence of each receptor. Every 10th residue is superscripted ' and every 100th, ". Beta strands for the growth hormone and prolactin receptors (de Vos et al., 1992; Somers et al., 1994) and the models are underlined. These β-strands are named A, B, C, C', E, F, and G in sequential order in each FnIII domain and are indicated above the strand, as is the hinge region, which connects the two FnIII domains. A detailed description of the secondary structure of GHR following the formalization of Kabsch and Sander (1983) is also given. The detailed codes used in the line GHR-2D are E, β-strand; G, 3_{10} helix; B, bridge; T, turn, S, backbone bend; *, β-bulge; and =, not seen in the electron density. Lowercase letters are used to indicate residues that flank secondary structural elements, either having only one hydrogen bond involved in a β-strand or having only one of their ϕ or ψ angles in the helical range. The strands in the models correspond well to the crystal structures except for the least well-conserved C strands, strand 2E, where a β-bulge in GHR disrupts the pattern, and the 2C and 2F strands in gp130, where the introduced β-bulge does not quite match the Kabsch and Sander (1983) criterion. Residues involved in growth hormone binding interactions (Clackson & Wells, 1995) are indicated by ^; tyrosine corners by ˇ; and residues that make up the "WSXWS" structural motif are marked ~. The alternative alignment of the first FnIII domain of the first CBD of LIFR is shown as DSCON in the figure. The symbol "*" in the DSCON sequence is used to indicate the insertion between the F and G strands needed to bring the alignment back into register.

This alignment, with the insertion in the FG loop indicated symbolically, is shown in Figure 1 as DSCON. The alternative to this is not to preserve the structural position of the second disulfide bridge. In this case, the disulfide bridge is placed between the C and C' strands and then the loop between the B and C strands is of normal length, a tyrosine corner motif is found between the E and F strands, and the loop between the F and G strands is of a more reasonable length. Also, this alignment (LIFRd1 in Fig. 1) shows a better pattern of amino acid conservation. Models using both positions for the second disulfide bridge were constructed and evaluated to test whether this novel disulfide arrangement was more probable in LIFR.

Because the growth hormone receptor is the only helical cytokine receptor structure for which coordinates are available (PDB code 3HHR; de Vos et al., 1992), it was used as the main template for the modeling. Other FnIII domains coordinates are available [Fibronectin 3rd domain, PDB code 1FNA (Dickinson et al., 1994); Tenascin 10th domain, 1TEN (Leahy et al., 1992); *Drosophila* neuroglian, 1CFB (Huber et al., 1994); tissue factor, 2HFT (Muller et al., 1994)], and these were examined as part of the alignment process and for structural similarity. It was found that, when the coordinates of these FnIII domains were superimposed, as shown in Figure 2, they had RMSD values ranging from 0.6 Å to 1.9 Å, with an average of 1.2 Å over the core B, C, E, and F strands (Smith, 1996). This surprisingly close structural similarity among the FnIII domains, despite their low sequence identity, justifies the use of these frameworks for the modeling of new receptor conformations.

A major consideration in the modeling of the LIF receptors is the determination of the angle between the two FnIII domains, whether this is conserved throughout the family, and whether it is likely to change on ligand binding or on interaction between the receptor subunits. The angle between the domains in the growth hormone receptor was used because the prolactin receptor domains (Somers et al., 1994) have essentially the same angle of about 90°, as do the structures of two EPO receptors bound to a synthetic ligand (Livnah et al., 1996). A similar pattern of conservation of the interdomain angle is found in the class II cytokine receptors. The interdomain angles seen in tissue factor in the free (Harlos et al., 1994; Muller et al., 1994) and ligand-bound (Banner et al., 1996) forms and in the interferon-γ receptor α-chain (Walter et al., 1995) are very similar and are about 120.

Model structural evaluation and refinement

The models built were examined for stereochemical quality using PROCHECK (Laskowski et al., 1993) at all stages of the refinement. Strained bond lengths and angles and out of plane aromatic and charged groups introduced by model construction were monitored and, if these did not correct themselves in the initial minimizations, they were constrained in the following refinement stages. Problems that tended to persist were caused by the fragment joints in the models, unfavorable ϕ–ψ angles where inserted loops originally contained Gly or Pro residues, and close side-chain contacts from residues substituted in inserted loops. Side-chain rotamers were sometimes unfavorable due to the way InsightII constructs side chains. The side-chain heavy atoms are preserved as far as possible during substitution and this can result in the transferred χ^1–χ^2 conformation being rare or unfavored for the substituted residue. If attempts to correct these problems introduced greater structural distortions, the restraint was redefined or removed and the refinement stage rerun. Because the final stage of the refinement was unrestrained (except for enhanced out-of-plane force constants—see Materials and methods), any structure maintained solely by these restraints would be revealed. After the unrestrained molecular dynamics and energy minimizations, the stereo chemical parameters of the models were (RMSDs from ideal values): bond angles, 2.5–3.9°; bond lengths, 0.1 Å; ω angle planarity, 3.5–4.0°; C^α tetrahedral distortion, 1.6–1.9°; most-favored regions of the ϕ–ψ plot, 67–77%; less-favored regions, 22–33%; additionally allowed regions, 0–3%; 1 residue in a "disallowed" high-energy region.

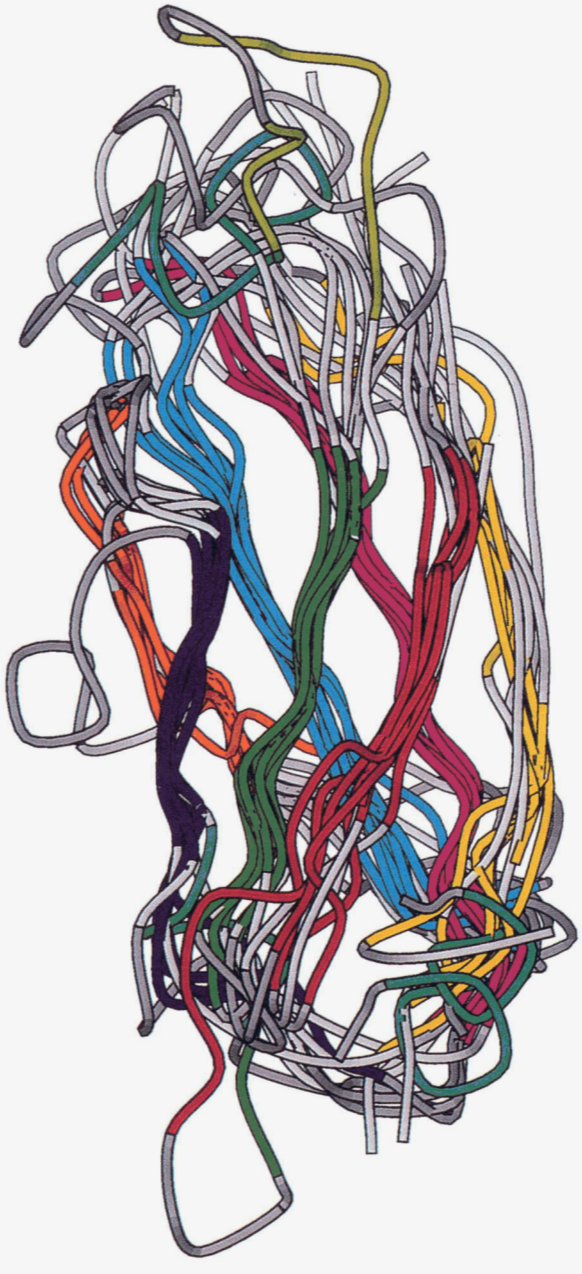

Fig. 2. MOLSCRIPT (Kraulis, 1991) diagrams of eight superimposed FnIII domains showing the close structural similarity. Structures depicted and their PDB codes are GHR (domains 1 and 2, 3HHR, chain B); tissue factor (domains 1 and 2, 2HFT); neuroglian (domains 1 and 2, 1CFB); fibronectin (1FNA); and tenascin (1TEN).

As well as stereochemical checks, the models were investigated with Profiles3D (Lüthy et al., 1992) and the empirical force field method, ProsaII (Sippl, 1993). On both measures, the models were comparable to the templates. For Profiles3D, the evaluation scores for the growth hormone receptors (de Vos et al., 1992) and *Drosophila* neuroglian (Huber et al., 1994) ranged from 69 to 81% (observed score/expected score) and for the models, values ranged from 63 to 79%. Similarly, when using ProsaII, the models scored slightly less well than the crystal structures overall, but were better than the experimental structures over considerable regions (Smith, 1996). The ProsaII graphs were below 0 (averaged over a window of 50), except for six residue values in the gp130 model and one in the model of the second CBD of LIFR. In these cases, no value exceeded +0.1. As an example, Figure 3 shows the typical progress of the refinement process as monitored by ProsaII for the model of the CBD of gp130. There is a general improvement, although it is not consistent, over the whole of the molecule. It was found during the refinement process that the evaluation methods were sensitive to small changes in the structure and that the two methods did not always agree on the merit of a particular structural change.

The alignments of the CBD of gp130 and the second CBD of LIFR (Fig. 1) were relatively unambiguous, but the alignment of the first CBD of LIFR was more complicated. Several variations of the alignment were considered and the models of these alignments were examined with ProsaII and Profiles to see if these methods indicated that one alignment was more suitable. Figure 4 shows the ProsaII trace of the model of the first CBD of LIFR with the second disulfide bridge in the standard position (Fig. 4A) and two variations of the models with the position of this disulfide bridge altered (Fig. 4B,C). The two alternative alignments of the second disulfide bridge in the first FnIII domain are shown in Figure 1 as LIFRd1 (cf. Fig. 4C) and DSCON (cf. Fig. 4A). Preserving the disulfide bridge position produced unsatisfactory scores in ProsaII for the model, as shown in Figure 4A. It was not possible to improve this with the techniques used in this study and, based on this and the sequence considerations mentioned above, further refinement of this model was not pursued. To achieve the final model using the alignment shown in Figure 1, several changes were made following examination of the ProsaII graphs. In the second FnIII domain of the CBD, the C to E strands were adjusted by two residues, giving a different packing of these strands. That is, the gap seen between strands 2B and 2C in the LIFRd1 sequence in Figure 1 was introduced, which required a correspond-

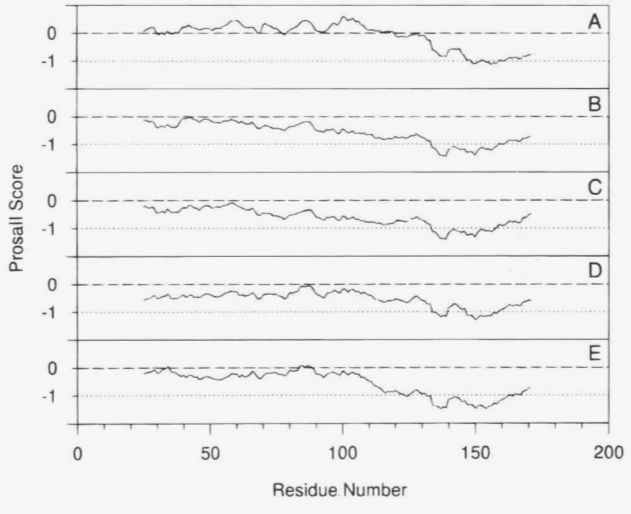

Fig. 3. ProsaII (Sippl, 1993) traces of the model of the gp130 CBD during its refinement. Values are averaged over a window of 50. **A:** Initial model. **B:** After energy minimizations. **C:** After molecular dynamics with the C^{α} atoms held fixed. **D:** After molecular dynamics with NOE hydrogen bond restraints. **E:** After unrestrained molecular dynamics. Native proteins are expected to be below the 0 line, which is shown dashed in each panel. Dotted line in each panel represents a score of −1. A general, but inconsistent, improvement has occurred throughout the refinement.

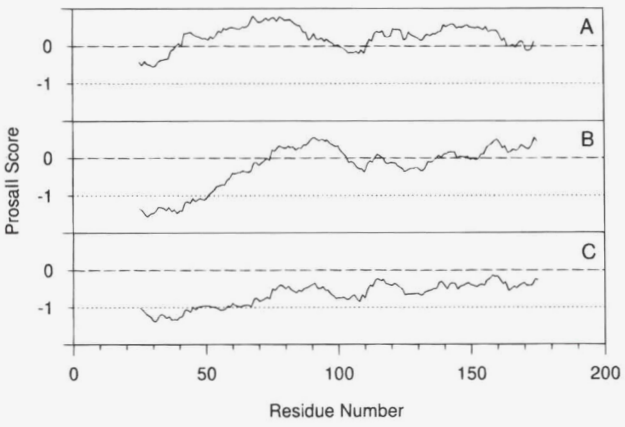

Fig. 4. Prosa II (Sippl, 1993) traces of models of the first CBD of LIFR. **A:** Model with the position of the second disulfide bridge conserved. **B,C:** Models with the position of the second disulfide bridge altered. B is a preliminary model, whereas C is the final model, which has an adjustment to the alignment of the C–E strand region of the second FnIII domain by two residues and the movement of a β-bulge from the C-terminus to the N-terminus of the G strand of the first FnIII domain (see alignments in Fig. 1).

ing insertion between strands 2D and 2E (Fig. 1). This resulted in the improvement of the ProsaII measure (a lowering of the values) for the C-terminal region (Fig. 4B,C). A second improvement was made in the G strand of the first FnIII domain by moving the β-bulge normally seen at the C-terminus of this strand to the N-terminus (see the alignments in Fig. 1). This caused two hydrophobic residues to align so that they packed into the β-sandwich rather than being exposed. Although this is another unique feature of the alignment of this CBD of LIFR, the improvement in the score from ProsaII (the lowering of the graph in Fig. 4C when compared to that in Fig. 4B), showing that this model is more compatible with features seen in native protein structures, suggests it is likely to be correct.

Electrostatic calculations

Using the parameters described in Materials and methods, electrostatic isopotential surfaces were calculated from the coordinates of the refined models. These were displayed using the program GRASP (Nicholls et al., 1991) at the ± 0.5 *kt/e* contour levels (blue positive, red negative) and are shown in Figure 5. The receptor CBDs are shown so that the putative receptor dimerization surface (by analogy to GHR) is in the plane of the page and the N-terminal FnIII domain is into the page. To dimerize, the receptors need to rotate by ± 90 toward each other (e.g., about the line between Fig. 5B,C). On the molecular surface of the second CBD of LIFR (Fig. 5A), the region expected to be involved in LIF binding (by analogy with GHR; Clackson & Wells, 1995; see Fig. 1) is shown in green and the region expected to form the receptor dimer contact region (by analogy with GHR; de Vos et al., 1992) is shown in magenta. If one of the CBDs of LIFR were to form a contact dimer with gp130 in the manner of the growth hormone receptor, then

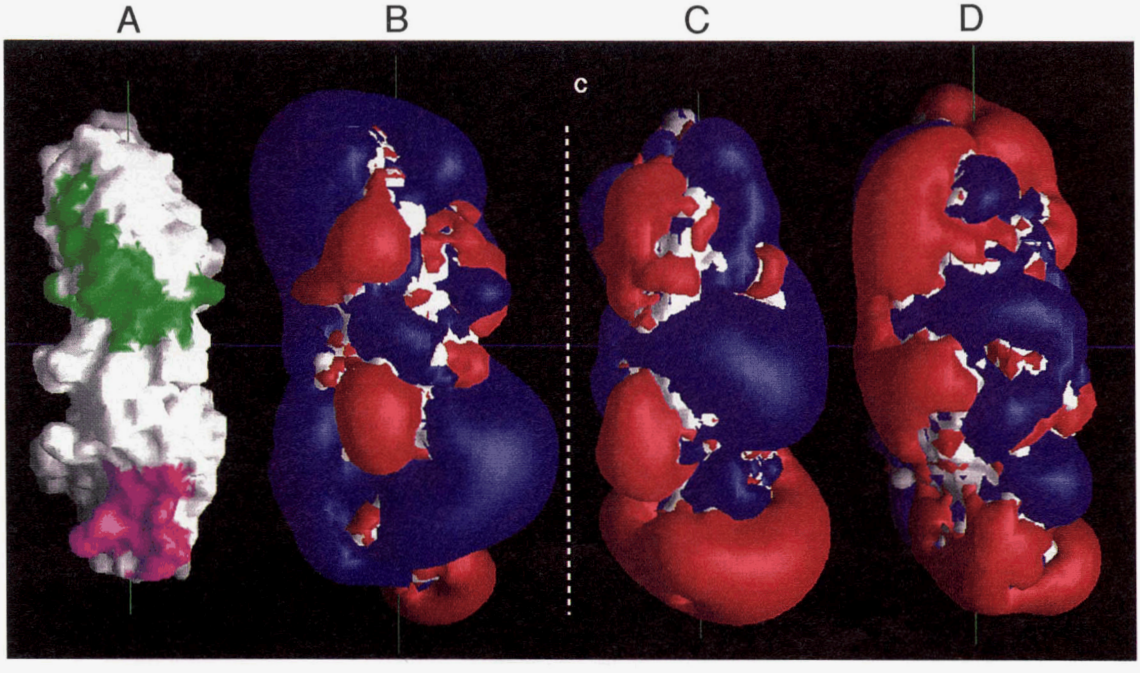

Fig. 5. Grasp (Nicholls et al., 1991) representations of the molecular and electrostatic isopotential surfaces of the models. **A:** Molecular surface of the model of the second CBD of LIFR. Areas marked in magenta and green show the residues equivalent to those involved in the dimer interface and in ligand interactions, respectively, of GHR. The putative dimer interface region is in the plane of the page and the binding site region is directed into the page. Electrostatic surfaces of the models are shown in (**B**) the second CBD of LIFR; (**C**) the CBD of gp130; and (**D**) the first CBD of LIFR. Blue regions are at $+0.5$ *kT/e* and red at -0.5 *kT/e*. To dimerize, the receptors must rotate toward each other by ± 90 about a line between them. Complementarity of the putative dimerization regions of the second CBD of LIFR (B), and the CBD of gp130 (C), is clear. The general similarity of the electrostatic profile of the first CBD of LIFR (D) to that of gp130 can be seen as well.

these receptors would be expected to have complementary electrostatic potentials in the proposed dimerization regions. Individually and when paired, the receptors would be expected to be electrostatically complementary to the binding regions on LIF.

From Figure 5 it can be seen that the models of the second CBD of LIFR and gp130 show clear electrostatic complementarity in the supposed dimerization region, whereas the model of the first CBD of LIFR does not. Instead, the electrostatic isopotential surface of the first CBD of LIFR looks very similar to that of gp130. To examine further the idea that the second CBD of LIFR and gp130 might be dimerization partners, their models were superimposed on the GHR dimer and their combined electrostatic potential surface, as well as that of LIF, was calculated. Figure 6 shows the resulting electrostatic isopotential surfaces. In this view, the ligand, LIF, has been rotated out of its potential binding region by 180, so that both binding surfaces are visible in the figure. The numbers marked on the ligand and the receptors show the regions of electrostatic complementarity between them that would be in contact if LIF bound these receptors following the growth hormone paradigm. The region marked Site I on LIF corresponds to the faces of the D and A helices and site II to the faces of the A and C helices and so are equivalent to the binding regions of growth hormone. These electrostatic surfaces suggest that the binding of LIF to the LIFR–gp130 complex follows the GH–GHR binding paradigm.

A possible third site for LIF binding has been identified (Layton et al., 1994b; Hudson et al., 1996). If the second CBD of LIFR and gp130 bind LIF following the GH–GHR paradigm, then it is likely that the first CBD of LIFR binds at Site III. It was hoped that the electrostatic profile of the model of this domain would indicate clear complementarity to the Site III region on LIF. However, the patterns of the positively and negatively charged regions were not sufficiently distinct to allow a definite prediction. Another hope of the electrostatic study of the first CBD of LIFR was that the isopotential surface might support a choice between the various alignments used by the model with the correct alignment having an electrostatic surface that was more clearly complementary to its binding partners. However, the electrostatic surface of the model with the position of the disulfide bridge in the first FnIII domain conserved and that of the model with the variation of the alignment in the second FnIII domain (data not shown) were not sufficiently different from the model shown in Figure 5D to use this method to choose among the models.

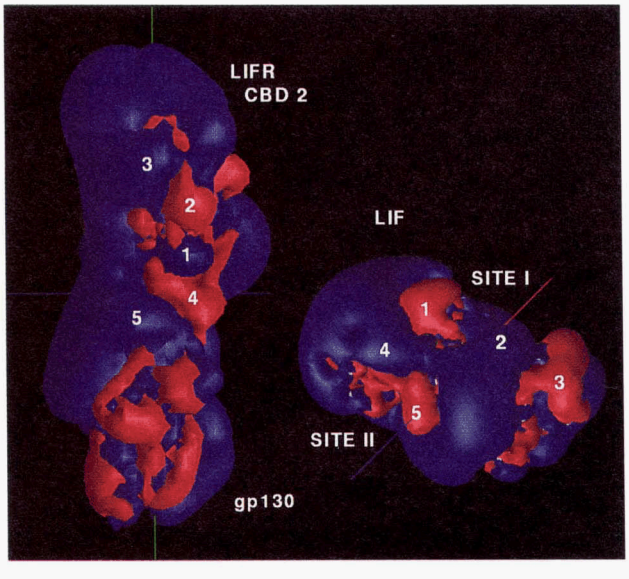

Fig. 6. Electrostatic surfaces as in Figure 4 of the second CDB of LIFR and the CBD of gp130, combined based on the GHR dimer, showing the ligand binding region and the electrostatic surface of LIF. Site I corresponds to the D and A helices and site II to the A and C helices. The numbered regions show the electrostatic complementarity between the ligand and the combined receptors.

Discussion

The LIFR is unusual among the helical cytokine receptors in that it has two CBDs that are separated by an Ig-like domain. Other receptors with two CBDs (e.g., the common β-chain and the interferon–receptor) have the CBDs adjoining each other, which would make it difficult on steric grounds for both CBDs to interact with the ligand. In these cases, the available data (Jenkins et al., 1995; Seto et al., 1995; Woodcock et al., 1996) suggest that the membrane-proximal CBD is involved in ligand interactions. With the separation of the CBDs in the LIF receptor by an Ig-like domain, interaction of both CBDs with LIF is not likely to be inhibited by steric clashes and both CBDs could bind LIF. Some data from other cytokine receptor systems have shown the involvement of receptor domains other than the CBD in ligand binding (IL-5R, Cornelis et al., 1995; G-CSFR, Hiraoka et al., 1995). However, in some receptors, the Ig-like domain has been shown to be unnecessary for binding (e.g., IL-6Rα, Yawata et al., 1993), which was initially thought to be the case for G-CSFR (Fukunaga et al., 1991), and the extracellular domains of many helical cytokine receptors contain only a CBD. In this work, models of both CBDs of the LIFR and the CBD of gp130 (the second component of the high-affinity LIF receptor complex, Gearing et al., 1992) were constructed, but not their Ig-like domains, to try to identify the locations where each of the CBDs might bind LIF and which of the CBDs, if any, might form contact dimers.

Evaluation of the models using stereochemical measures (PROCHECK, Laskowski et al., 1993) and estimates of their compatibility with the characteristics of known protein structures (ProsaII, Sippl, 1993; Profiles3D, Lüthy et al., 1992) showed them to be of equivalent quality to the template molecules used in their construction. Use of these evaluation methods suggested an alteration by two residues to the alignment of the second FnIII domain of the first CBD of LIFR. A misalignment of two residues in β-sandwich proteins can be made easily, because the pattern of alternating hydrophobic–hydrophilic residues will be maintained although the β-strand length will alter. Another alignment change suggested by the evaluation of the models was to move a β-bulge to the opposite end of the strand from which it appears in the other receptors (Fig. 1). The considerable improvement in the evaluation score of the model given this adjustment suggests the appropriateness of this alteration. However, the methods used in this work do not allow an unambiguous evaluation of the correctness of this and experimental data will be needed to confirm the alignments.

Part of the aim of this work was to examine the usefulness of the electrostatic surfaces of homology models. The importance of electrostatic interactions in helical cytokine–receptor interactions has been shown by mutagenesis studies (Lopez et al., 1992; Cunningham & Wells, 1993; Kruse et al., 1993; Zurawski et al., 1993; Clackson & Wells, 1995; Graber et al., 1995; Olins et al., 1995) and the electrostatic complementarity of GH to its receptors has

also been described (Demchuk et al., 1994; Layton et al., 1997). In the case of the LIF receptor complex, the models of the second CBD of LIFR and the CBD of gp130 showed a very clear electrostatic complementarity over the region that would be expected to dimerize if the complex formed in a manner similar to that of GH–GHR (Fig. 5B,C). This suggests that these molecules will dimerize, thereby forming a binding region for LIF that should show electrostatic complementarity to LIF. When the electrostatic isopotential surface of LIF was calculated, the surface formed by the region encompassing the D-A-C helices (equivalent to Sites I and II of GH) was complementary to the surface of the combined receptors (Fig. 6). Taken together, these data provide strong evidence that LIF does follow the growth hormone paradigm of cytokine binding. The second CBD of LIFR would appear to bind to the D and A helices (equivalent to Site I of GH) and then gp130 appears to bind to the A and C helices (equivalent to site II of GH) while forming a contact dimer with LIFR. This model follows the emerging pattern of cytokine binding (Mott & Campbell, 1995) and is also consistent with the available mutagenesis data on LIF (Layton et al., 1994b; Hudson et al., 1996), which is summarized in Figure 7 and discussed below.

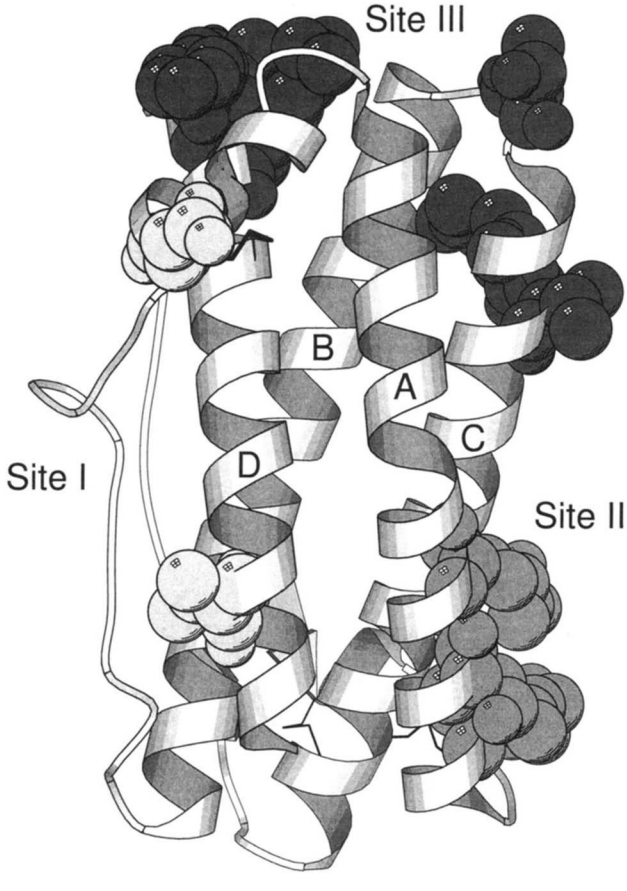

Fig. 7. MOLSCRIPT diagram (Kraulis, 1991) of the crystal structure of murine LIF (Robinson et al., 1994) showing the three binding site regions and the residues identified by Layton et al. (1994b) and Hudson et al. (1996) as affecting receptor binding. Residues of murine LIF equivalent to those identified for human LIF are shown. Site I residues (Glu^{57}, Val^{175}) are in light gray, site II residues (Gln^{25}, Asn^{28}, Gln^{32}) are in medium gray, and site III residues (Thr^{107}, Gln^{112}, Val^{113}, Ala^{155}, Phe^{156}, Arg^{158}, Lys^{159}) are in dark gray.

The putative dimerization region of the first CBD of LIFR was not electrostatically complementary to gp130 and would not be expected to dimerize with gp130 or bind LIF following the GH–GHR paradigm. Unexpectedly, it was noted that its potential dimerization region had an electrostatic profile that was very similar to that of gp130. This raises the possibility that this CBD might dimerize with other receptors to which gp130 also forms dimers. In particular, it may be that this domain is the part of LIFR that is involved in binding CNTF where one LIFR molecule and one gp130 molecule are involved in an IL-6-like hexameric complex (de Serio et al., 1995). This could explain the apparently anomalous role of LIFR in this complex and will be discussed in more detail elsewhere in the context of gp130-related receptor complexes (Smith, 1996; D.K. Smith, A. Hammacher, & H.R. Treutlein, manuscript in prep.).

Because it could not be predicted confidently from the electrostatic surfaces that the first CDB of LIFR would bind to site III on LIF, another possibility might be that the Ig-like domain of the receptor or the interface between the Ig-like domain and the first CBD could interact with LIF. The recent cloning of a second OSM receptor (Mosley et al., 1996), which is like LIFR but lacks the first FnIII domain of the first CBD, might possibly argue for this. However, if the second CBD of LIFR and gp130 bind LIF as suggested above (Fig. 6), it seems unlikely, on steric grounds, that the Ig-like domain could bind to LIF. The Ig-like domain might spatially separate and orient the first CBD to allow it to be placed in position to bind at site III. It is possible to test this by constructing a deletion mutant of LIFR that lacks the N-terminal FnIII domain. If the Ig-like domain is directly involved in ligand interactions, this mutant should have relatively little effect on binding, whereas, if the first CBD binds LIF directly, the effect of this mutant should be considerable. Alterations to the Ig-like domain or mutations in the interface between the Ig-like domain and the CBD need to be evaluated carefully, because they may affect the ability of the first CBD of LIFR to orient correctly toward site III rather than suggesting a different binding mode.

The biochemical data available on LIF–receptor interactions include mutagenesis and cross species binding and competition studies. Indicated in Figure 7, a ribbon diagram (Kraulis, 1991) of the crystal structure of murine LIF (Robinson et al., 1994), are the locations of the three binding sites, with the residues identified by the studies described below shown in CPK form. Owczarek et al. (1993) and Layton et al. (1994b) used chimeric protein studies to identify six residues of human LIF that, when substituted into murine LIF, gave murine LIF binding and biological activity similar to that of human LIF. Five of these residues localize to the region described as site III, whereas the sixth, Asp^{57}, in the small helix in the AB loop, co-localizes with Site I residues seen in GH (Cunningham & Wells, 1993). Other residues that co-localize with Site I were shown to affect LIFR binding (Hudson et al., 1996). Groups of residues on the A and C helices (co-localizing with Site II), when co-mutated to Ala, were shown to affect gp130 binding with the A helix residues having a greater effect (Hudson et al., 1996). The residues identified by Hudson et al. (1996) as having the greatest effect on LIF receptor binding were Phe^{156} and Lys^{159}. Phe^{156} is involved in a structural interaction between the "D1 motif" and the small helix in the AB loop (Pro^{51}, Phe^{52}, and Leu^{59}) and this interaction probably contributes to the stability of the "D1 motif" as part of Site III and therefore may not directly contribute to binding (Smith, 1996; Simpson et al., 1997). Lys^{159} is partly exposed on the same face of LIF as the five site III

residues identified by Layton et al. (1994b) and may contribute directly to binding; the equivalent residue in CNTF, Lys^{155}, was shown to considerably affect LIFR binding to CNTF (di Marco et al., 1996). However, in the crystal structures of both LIF (Robinson et al., 1994) and CNTF (McDonald et al., 1995), it can be seen that the aliphatic part of the Lys side chain is buried (Lys^{159} in LIF makes close contacts with Phe^{52}) and is likely to structurally stabilize this region of the molecules. Overall, the residues identified in these studies (Owczarek et al., 1993; Layton et al., 1994b; Hudson et al., 1996) as affecting receptor binding are consistent with the receptor complex model proposed here.

The models of the second CBD of LIFR and gp130 and the crystal structure of murine LIF (Robinson et al., 1994) were superimposed on the GH–GHR complex to examine how the models might explain the mutagenesis data of Hudson et al. (1996) and Layton et al. (1994b). Residues thought to be involved in site III interactions cannot be commented on further due to the inability to precisely define a binding region for the first CBD of LIFR. For the residues likely to be in site I in LIF that were found not to affect LIFR interactions (Hudson et al., 1996), Gln^{178} appeared to be beyond the contact area, Ala^{177} was directed toward the cleft between the two receptors, Gln^{171} was at the upper fringe of the binding area (as in the receptor view in Fig. 6), and the residues from Ala^{61} to Thr^{65} were above the binding region. Of the residues in LIF that affected receptor binding, Val^{175} and Lys^{170} were in the contact region with LIFR, however, Asp^{57} and Lys^{58} were distant from the receptor. Residues on the receptor that are involved in ligand contacts come from the loop regions. These loops are named by the strand names, given in Figure 1, that flank them and by the number of the FnIII domain (1 or 2, Fig. 1) that they are in. In the second CBD of LIFR, the residues in contact with LIF are Leu^{302} (1AB loop), Gln^{359} (1EF loop), Thr^{384} (hinge region), Lys^{417} and Asn^{419} (2BC loop), and Thr^{471} and Phe^{472} (2FG loop).

From the electrostatic surfaces in Figure 6, it seems possible that LIF might bind its receptors from a position on the helices farther from the N- and C-termini than that suggested by the optimal superposition of LIF and GH (residues 21, 77, 125, and 170 of LIF equivalent to 8, 73, 117, and 167 of GH, respectively) used above. Accordingly, a superposition of residues 28, 84, 118, and 163 of LIF to the GH residues mentioned above was examined to see how this matched the mutagenesis data. In this case, Asp^{57} and Lys^{58} in LIF were able to make contacts with the receptor. Asp^{57} was close to Lys^{472} (2EF loop, LIFR) and Lys^{58} could be close to Glu^{385} (hinge region, LIFR) if, in solution, the side chain of Lys^{58} folds back to the surface of LIF rather than protruding from the molecule as seen in the crystal structure. Most notable of the other residues in LIF was that Gln^{171}, which had a slight effect on LIFR binding (Hudson et al., 1996), was in the interface between the two molecules. This might be explained by Lys^{417} (2BC loop, LIFR) appearing to make a hydrogen bond to its backbone carbonyl group. Because this bond would not be affected by the mutation $Gln^{171}Ala$, this could ameliorate the apparent loss of contacts from the side chain. Val^{175} and Lys^{170} in LIF were still in contact with the receptor and, although the region from Ala^{61} to Thr^{65} in LIF was closer to the receptor in this superposition, it was still at the top edge of the interface region.

In the case of site II interactions, the residues identified by Hudson et al. (1996) in the A helix of LIF made contacts with gp130, whereas the residues in the C helix were generally above the contact region and consequently would be expected to have less effect on gp130 binding, as found by Hudson et al. (1996). In the initial superposition, Ser^{36} and Ala^{117} of LIF were at the edge of the binding region and unlikely to contribute greatly to binding, whereas the residues of LIF identified as making the main contribution, Gln^{25}, Ser^{28}, and Gln^{32} (Hudson et al., 1996), formed contacts with the following residues in gp130: Tyr^{168} and Phe^{169} (1EF loop), Val^{195} and Tyr^{196} (hinge region), Lys^{218} and Val^{220} (2BC loop), and Lys^{275} (2FG loop). When the superposition was altered, Ser^{36} and Ala^{117} of LIF became closer to the binding region, whereas Gln^{25} was more to the edge. An examination of the electrostatic surfaces of LIF and the receptors, as shown in Figure 6, suggests that LIF might be angled across the receptors in a slightly different manner to GH. In this case, the initial superposition of LIF on GH would be more suitable for the gp130 interaction and the second superposition would be more appropriate for the LIFR interaction. The receptor–dimer interface suggested by the electrostatic surfaces of the receptor models is dominated by the charged residues Lys^{396} and Lys^{398} (2A strand), Lys^{406} (2B strand), and Asp^{453} (2E strand) in LIFR, and by Glu^{212} and Glu^{213} (2A strand), Lys^{219} (2B strand), and Asp^{366} (2E strand) in gp130.

Other studies on LIFR binding have shown a complex pattern of receptor binding (Layton et al., 1994a). Human LIF shows biphasic dissociation from its cognate receptor, whereas human and murine LIF show monophasic dissociation from murine LIFR (Layton et al., 1994a). Further, both human and murine LIF are less effective competitors against the cross species ligand when binding to murine LIFR than would be expected from their respective individual binding affinities (Layton et al., 1994a). From the binding pattern suggested by the models here and the mutagenesis data, the dissociation behavior can be explained by there being two binding sites for LIFR. Monophasic dissociation may be observed if one binding site has a much greater affinity than the other or if binding at one site is dependent on binding at the other, as is the case for the IL-6Rα-dependent binding of gp130 to IL-6 (Paonessa et al., 1995). The interaction involving Phe^{156}, noted above, may provide a mechanism for this in LIF by structurally linking the AB loop (Site I) and the D helix (Site III) (Smith, 1996; Simpson et al., 1997). Biphasic dissociation will occur if the sites are not completely dependent, so that binding might occur at either site and if the dissociation constants of the sites are somewhat different. Slight structural differences between human and murine LIF and their receptors and a possibly stronger site III interaction in human LIF (discussed below) may cause the different observed dissociation behavior through these mechanisms.

The growth hormone style of receptor binding suggested by the modeling implies that the second CBD of LIFR is more important for ligand binding, because it will dimerize with gp130 to allow signaling, and so it is likely that LIF first associates with the second CBD. Most of the residues, identified by Layton et al. (1994b), which convert murine LIF binding to human-like behavior, cluster in the site III region and, based on the modeling, will interact with the first CBD. Therefore, it is probable that the (nonnative) strong binding of human LIF to murine LIFR is dominated by site III interactions and that human LIF binds initially to the first CBD of murine LIFR. Consequently, the unexpected heterologous competition may be explained by murine LIF initially associating on the second CBD of murine LIFR, whereas the nonnative association of human LIF is being initiated on the first CBD. Thus, the two molecules could inhibit the binding of the other, an effect that would not be observed in homologous competition because both competitors would utilize the same initial site. The

apparent strong binding interaction of site III on human LIF to murine LIFR might suggest that this site forms a stronger native interaction in the human system than in the murine system, perhaps explaining the different cross species dissociation behavior. A recent study of chimeric LIF receptors (Owczarek et al., 1997) has also postulated that the second CBD of LIFR might play a more dominant role than the first CBD, consistent with the suggestion from the modeling that the second CBD of LIFR is involved in a GHR-like interaction. The effect of the Ig-like domain that they observe might be more consistent with an alteration of the orientation of the CBDs, as noted above, rather than the possibility of ligand–Ig-like domain contacts that they suggest (Owczarek et al., 1997). The modeling also suggests that the complex of LIF and its receptors will be trimeric, which is supported by the recent study of Zhang et al. (1997).

In summary, the LIFR and gp130 models are consistent with the stereochemical parameters of proteins and with the structural principles seen in native proteins. The means used to evaluate the compatibility of the models with native structures (ProsaII, Sippl, 1993; Profiles3D, Lüthy et al., 1992) were able to suggest some improvements to the sequence alignments used to build the models. Electrostatic analyses of the receptor models enabled binding partners to be inferred based on the complementarity of the electrostatic surfaces of the ligand and the receptors. These data strongly support a binding mode for LIF, following the growth hormone paradigm, in which the second CBD of LIFR binds to site I (the D and A helices) and then dimerizes with gp130, which binds to site II (the A and C helices). This proposed LIF–receptor complex is consistent with the mutagenesis and binding data that are currently available. Unfortunately, the electrostatic analyses were not able to define the site III binding region more precisely nor to allow a choice between models based on slightly different alignments. The models described here have provided strong evidence that, like other cytokines, LIF follows the growth hormone paradigm of helical cytokine binding to sites I and II and have further demonstrated the utility of electrostatic surfaces for predicting domain interactions from homology models. Our modeling results suggest regions on both receptors that can be investigated further by mutagenesis or deletion mutants.

Materials and methods

Sequence alignments

CBD sequences were aligned by predominately manual means, taking into account pronounced sequence features such as the conserved disulfide bridges, the proline-rich linker between the two FnIII domains, tyrosine corners (Hemmingsen et al., 1994), the "WSXWS" motif, the alternating pattern of hydrophobic–hydrophilic residues seen in β-sandwich proteins, and the secondary structure of the human growth hormone receptor (de Vos et al., 1992). Several different species of the growth hormone receptor, the prolactin receptor, the granulocyte colony-stimulating factor receptor, and the IL-6 receptor, as well as gp130 and LIFR, were used to provide a more detailed basis for the alignment. The sequences of the CBDs of LIFR are somewhat unusual, which complicated the alignment process. In the membrane-proximal (or "second") CBD of LIFR, the second of the two "conserved" disulfide bridges is missing, whereas, in the N-terminal (or "first") CBD, although the four cysteine residues are present, considerable sequence insertions and deletions are required if the third and fourth cysteine residues are to be aligned with those in the other sequences. Due to the apparently strong conservation of the second disulfide bridge in the class 1 helical cytokine receptors, alignments that preserved and altered the position of the second disulfide bridge were used to model this domain.

Model building and refinement

Models based on the alignments were constructed using the Homology module of InsightII (Molecular Simulations Inc., San Diego, California). The coordinates of the site I growth hormone receptor (chain B of PDB entry 3HHR) were used as a template for the β-sheet regions of the receptors and for some of the loops where the lengths matched. Other loops were taken from the structures of FnIII domains or from a search of the PDB (Bernstein et al., 1977). Once coordinates had been created, the models were refined using the X-PLOR program (Brünger, 1992). In general, the refinement process followed the simulated annealing and molecular dynamics in water procedure using the OPLS force field (Jorgensen & Tirado-Rives, 1988) as described by Smith et al. (1994). Initially, the models were subjected to energy minimizations in vacuo with no electrostatic term and only a repulsive van der Waals term. The first minimizations held the backbone atoms fixed and subsequently the splice joints of the models were released and further minimized with a final round of minimizations holding only the C^{α} atoms fixed. Following this, the models were surrounded with a 5-Å layer of water molecules and subjected to simulated annealing and molecular dynamics. This was performed for two restrained stages, one with the C^{α} atoms held fixed and another where backbone hydrogen bond constraints were simulated using NOE style restraints. Hydrogen bonds were inferred from the growth hormone receptor structure and an upper bound of 2.2 Å on the O-H distance was used so that the secondary structure was maintained while allowing the backbone to flex. During these two stages, restraints were placed on peptide bond planarity, C^{α} tetrahedral distortion, and out-of-plane distortions of aromatic ring and charged side-chain groups. Due to an inadequacy with out-of-plane distortions in the OPLS force field (Cornell et al., 1995), this constraint was maintained throughout the refinement process. Additional restraints were used to correct some backbone bond and dihedral angles that had formed abnormal values in the model-building process. These restraints were monitored throughout the refinement process and altered or removed as necessary. The final stage of the refinement process was unrestrained (except for the out-of-plane force) molecular dynamics in water for 50 ps at 300 K.

Structure validation

The models were examined for stereochemical quality by the use of the PROCHECK suite of programs (Laskowski et al., 1993). Further tests of the quality of the models were made using the Profiles3D method (Bowie et al., 1991; Lüthy et al., 1992) as implemented in InsightII and the empirical force field method implemented in ProsaII (Hendlich et al., 1990; Sippl, 1993). Where these programs indicated problems in the models, the restraints used in the refinement process were either applied, adjusted, or removed and the refinement restarted. In some cases, alternative alignments were tried and the models rebuilt.

Electrostatic calculations

Calculations of the electrostatic isopotential surfaces of the models followed the general principle described by Demchuk et al. (1994). Potential maps were constructed using the program DelPhi (Gilson et al., 1988; Nicholls & Honig, 1991). Grid sizes of both 65^3 and 129^3 were used and the molecule's position on the grid was varied. These changes did not alter the results significantly. Parameters used in the calculation were: a probe radius of 1.4 Å, an ion exclusion layer of 2.0 Å, a salt concentration of 0.145 M, standard van der Waals radii, partial charges from the OPLS force field (Jorgensen & Tirado-Rives, 1988), a solvent dielectric of 80, and a solute dielectric of 2. Histidine residues were treated as having a net charge of +0.5 *e*. Visualization of the electrostatic surfaces was achieved using the program GRASP (Nicholls et al., 1991).

Acknowledgments

D.K.S. was supported in part by a University of Melbourne special scholarship, funded by the Victorian Education Foundation. Prof. A.W. Burgess is thanked for a critical review of the manuscript and Drs. A. Hammacher, C.M. Owczarek, and M.J. Layton are thanked for helpful discussions.

References

Banner DW, D'arcy A, Chène C, Winkler FK, Guha A, Konigsberg WH, Nemerson Y, Kirchhofer D. 1996. The crystal structure of the complex of blood coagulation factor VIIa with soluble tissue factor. *Nature 380*:41–46.

Bazan JF. 1990. Structural design and molecular evolution of a cytokine receptor superfamily. *Proc Natl Acad Sci USA 87*:6934–6938.

Bazan JF. 1991. Neuropoietic cytokines in the hematopoietic fold. *Neuron 7*:197–208.

Bernstein FC, Koetzle TF, Williams GJB, Meyer EF Jr, Brice MD, Rodgers JR, Kennard O, Shimanouchi T, Tasumi M. 1977. The Protein Data Bank: A computer-based archival file for macromolecular structures. *J Mol Biol 112*:535–542.

Bowie JU, Lüthy R, Eisenberg D. 1991. A method to identify protein sequences that fold into a known three-dimensional structure. *Science 253*:164–170.

Brünger AT. 1992. *X-PLOR, a system for crystallography and NMR*. New Haven, Connecticut: Yale University.

Cheema SS, Richards L, Murphy M, Bartlett PF. 1994. Leukemia inhibitory factor prevents the death of axotomised sensory neurons in the dorsal root ganglia of the neonatal rat. *J Neurosci Res 37*:213–218.

Chua AO, Chizzonite R, Desai BB, Truitt TP, Nunes P, Minetti LJ, Warrier RR, Presky DH, Levine JF, Gately MK, Gubler U. 1994. Expression cloning of a human IL-12 receptor component. *J Immunol 153*:128–136.

Clackson T, Wells JA. 1995. A hot spot of binding energy in a hormone–receptor interface. *Science 267*:383–386.

Cornelis S, Plaetinck G, Devos R, Van der Heyden J, Tavernier J, Sanderson CJ, Guisez Y, Fiers W. 1995. Detailed analysis of the IL-5–IL-5R interaction: Characterization of crucial residues on the ligand and the receptor. *EMBO J 14*:3395–3402.

Cornell WD, Cieplak P, Bayly CI, Gould IR, Merz KM, Ferguson DM, Spellmeyer DC, Fox T, Caldwell JW, Kollman PA. 1995. A second generation force field for the simulation of proteins, nucleic acids, and organic molecules. *J Am Chem Soc 117*:5179–5197.

Cosman D. 1993. The hematopoietin receptor superfamily. *Cytokin 5*:95–106.

Cunningham BC, Ultsch M, de Vos AM, Mulkerrin MG, Clauser KR, Wells JA. 1991. Dimerization of the extracellular domain of the human growth hormone receptor by a single hormone molecule. *Science 254*:821–825.

Cunningham BC, Wells JA. 1993. Comparison of a structural and a functional epitope. *J Mol Biol 234*:554–563.

Demchuk E, Mueller T, Oschkinat H, Sebald W, Wade RC. 1994. Receptor binding properties of four-helix-bundle growth factors deduced from electrostatic analysis. *Protein Sci 3*:920–935.

de Serio A, Graziani R, Laufer R, Ciliberto G, Paonessa G. 1995. In vitro binding of ciliary neurotrophic factor to its receptors: Evidence for the formation of an IL-6-type hexameric complex. *J Mol Biol 254*:795–800.

de Vos AM, Ultsch M, Kossiakoff AA. 1992. Human growth hormone and extracellular domain of its receptor: Crystal structure of the complex. *Science 255*:306–312.

Dickinson CD, Veerapandian B, Dai XP, Hamlin RC, Xuong N, Ruoslahti E, Ely KR. 1994. Crystal structure of the tenth type III cell adhesion module of human fibronectin. *J Mol Biol 236*:1079–1092.

di Marco A, Gloaguen I, Graziani R, Paonessa G, Saggio I, Hudson KR, Laufer R. 1996. Identification of ciliary neurotrophic factor (CNTF) residues essential for leukemia inhibitory factor receptor binding and generation of CNTF antagonists. *Proc Natl Acad Sci USA 93*:9247–9252.

Fukunaga R, Ishizaka-Ikeda E, Pan CX, Seto Y, Nagata S. 1991. Functional domains of the granulocyte colony-stimulating factor receptor. *EMBO J 10*:2855–2865.

Gearing DP, Comeau MR, Friend DJ, Gimpel SD, Thut CJ, McGourty J, Brasher KK, King JA, Gillis S, Mosley B, Ziegler SF, Cosman D. 1992. The IL-6 signal transducer, gp130: An oncostatin M receptor and affinity converter for the LIF receptor. *Science 255*:1434–1437.

Gearing DP, Thut CJ, van den Bos T, Gimpel SD, Delaney PB, King J, Price V, Cosman D, Beckmann MP. 1991. Leukemia inhibitory factor receptor is structurally related to the IL-6 signal transducer, gp130. *EMBO J 10*:2839–2848.

Gilson MK, Sharp KA, Honig BH. 1988. Calculating the electrostatic potential of molecules in solution: Method and error assessment. *J Comp Chem 9*:327–335.

Graber P, Proudfoot AEI, Talabot F, Bernard A, McKinnon M, Banks M, Fattah D, Solari R, Peitsch MC, Wells TNC. 1995. Identification of key charged residues of human interleukin-5 in receptor binding and cellular activation. *J Biol Chem 270*:15762–15769.

Harlos K, Martin DMA, O'Brien DP, Jones EY, Stuart DI, Polikarpov I, Miller A, Tuddenham EGD, Boys CWG. 1994. Crystal structure of the extracellular region of human tissue factor. *Nature 370*:662–666.

Hemmingsen JM, Gernert KM, Richardson JS, Richardson DC. 1994. The tyrosine corner: A feature of most Greek key β-barrel proteins. *Protein Sci 3*:1927–1937.

Hendlich M, Lackner P, Weitckus S, Floeckner H, Froschauer R, Gottsbacher K, Casari G, Sippl MJ. 1990. Identification of native protein folds amongst a large number of incorrect models. *J Mol Biol 213*:859–883.

Hilton DJ. 1992. LIF: Lots of interesting functions. *Trends Biochem Sci 17*: 72–76.

Hiraoka O, Anaguchi H, Asakura A, Ota Y. 1995. Requirement for the immunoglobulin-like domain of granulocyte colony-stimulating factor receptor in formation of a 2:1 receptor-ligand complex. *J Biol Chem 270*:25928–25934.

Huber AH, Eureka Wang Y, Bieber AJ, Bjorkman PJ. 1994. Crystal structure of tandem type III fibronectin domains from *Drosophila* neuroglian at 2.0 Å. *Neuron 12*:717–731.

Hudson KR, Vernallis AB, Heath JK. 1996. Characterization of the receptor binding sites of human leukemia inhibitory factor and creation of agonists. *J Biol Chem 271*:11971–11978.

Jenkins BJ, D'Andrea R, Gonda TJ. 1995. Activating point mutations in the common subunit of the human GM-CSF, IL-3 and IL-5 receptors suggest the involvement of subunit dimerization and cell type-specific molecules and signalling. *EMBO J 17*:4276–4287.

Jorgensen WL, Tirado-Rives J. 1988. The OPLS potential functions for proteins. Energy minimisations for crystals of cyclic peptides and crambin. *J Am Chem Soc 110*:1657–1666.

Kabsch W, Sander C. 1983. Dictionary of protein secondary structure: Pattern recognition of hydrogen-bonded and geometric features. *Biopolymers 22*: 2577–2637.

Kishimoto T, Akira S, Narazaki M, Taga T. 1995. Interleukin-6 family of cytokines and gp130. *Blood 86*:1243–1254.

Kraulis P. 1991. MOLSCRIPT: A program to produce both detailed and schematic plots of protein structures. *J Appl Crystallogr 24*:946–950.

Kruse N, Shen BJ, Arnold S, Tony HP, Müller T, Sebald W. 1993. Two distinct functional sites of human interleukin 4 are identified by variants impaired in either receptor binding or receptor activation. *EMBO J 12*:5121–5129.

Laskowski RA, MacArthur MW, Moss DS, Thornton JM. 1993. PROCHECK: A program to check the stereochemical quality of protein structures. *J Appl Crystallogr 26*:283–291.

Layton JE, Iaria J, Smith DK, Treutlein HR. 1997. Identification of a ligand binding site on the granulocyte colony-stimulating factor receptor by molecular modeling and mutagenesis. *J Biol Chem 272*: 29735–29741.

Layton MJ, Lock P, Metcalf D, Nicola NA. 1994a. Cross-species receptor binding characteristics of human and mouse leukemia inhibitory factor suggest a complex binding interaction. *J Biol Chem 269*:17048–17055.

Layton MJ, Owczarek CM, Metcalf D, Clark RL, Smith DK, Treutlein HR, Nicola NA. 1994b. Conversion of the biological specificity of murine to human leukemia inhibitory factor by replacing 6 amino acid residues. *J Biol Chem 269*:29891–29896.

Leahy DJ, Hendrickson WA, Aukhil I, Erickson HP. 1992. Structure of a fibronectin type III domain from Tenascin phased by MAD analysis of the selenomethionyl protein. *Science 258*:987–991.

Li M, Sendtner M, Smith A. 1995. Essential function of LIF receptor in motor neurons. *Nature 378*:724–727.

Livnah O, Stura EA, Johnson DL, Middleon SA, Mulcahy LS, Wrighton NC, Dower WJ, Jolliffe LK, Wilson IA. 1996. Functional mimicry of a protein hormone by a peptide agonist: The EPO receptor complex at 2.8. *Science 273*:464–471.

Lopez AF, Shannon MF, Hercus T, Nicola NA, Cambareri B, Dottore M, Layton MJ, Eglinton L, Vadas MA. 1992. Residue 21 of human granulocyte-macrophage colony-stimulating factor is critical for biological activity and for high but not low affinity binding. *EMBO J 11*:909–916.

Lüthy R, Bowie JU, Eisenberg D. 1992. Assessment of protein models with three-dimensional profiles. *Nature 356*:83–85.

McDonald NQ, Panayolatos N, Hendrickson WA. 1995. Crystal structure of dimeric human ciliary neurotrophic factor determined by MAO phasing. *EMBO J 14*: 2689–2699.

Metcalf D. 1992. Leukemia inhibitory factor—A puzzling polyfunctional regulator. *Growth Factors 7*:169–173.

Mosley B, de Imus C, Friend D, Boiani N, Thoma B, Park LS, Cosman D. 1996. Dual Oncostatin M (OSM) receptors. Cloning and characterization of an alternative signalling subunit conferring OSM-specific receptor activation. *J Biol Chem 271*:32635–32643.

Mott HR, Campbell ID. 1995. Four-helix bundle growth factors and their receptors: Protein–protein interactions. *Curr Opin Struct Biol 5*:114–121.

Muller YA, Ultsch MH, de Vos AM. 1996. The crystal structure of the extracellular domain of human tissue factor refined to 1.7 Å resolution. *J Mol Biol 256*:144–159.

Muller YA, Ultsch MH, Kelley RF, de Vos AM. 1994. Structure of the extracellular domain of human tissue factor: Location of the factor VIIa binding site. *Biochemistry 33*:10864–10870.

Nicholls A, Honig B. 1991. A rapid finite difference algorithm, utilizing successive over-relaxation to solve the Poisson–Boltzmann equation. *J Comp Chem 12*:435–445.

Nicholls A, Sharp KA, Honig BH. 1991. Protein folding and associations: Insights from the interfacial and thermodynamic properties of hydrocarbons. *Proteins Struct Funct Genet 11*:281–296.

Olins PO, Bauer SC, Bradford-Goldberg S, Sterbenz K, Polazzi JO, Caparon MH, Klein BK, Easton AM, Paik K, Klover JA, Thiele BR, McKearn JP. 1995. Saturation mutagenesis of human Interleukin-3. *J Biol Chem 270*: 23754–23760.

Owczarek CM, Layton MJ, Metcalf D, Lock P, Willison TA, Gough NM, Nicola NA. 1993. Inter-species chimeras of leukaemia inhibitory factor define a major human receptor-binding determinant. *EMBO J 12*:3487–3495.

Owczarek CM, Zhang Y, Layton MJ, Metcalf D, Roberts B, Nicola NA. 1997. The unusual species cross-reactivity of the leukemia inhibitory factor receptor α-chain is determined primarily by the immunoglobulin-like domain. *J Biol Chem 272*:23976–23985.

Paonessa G, Graziani R, de Serio A, Savino R, Ciapponi L, Lahm A, Salvati AL, Toniatti C, Ciliberto G. 1995. Two distinct and independent sites on IL-6 trigger gp130 dimer formation and signalling. *EMBO J 9*:1942–1951.

Patterson PH. 1994. Leukemia inhibitory factor, a cytokine at the interface between neurobiology and immunology. *Proc Natl Acad Sci USA 91*:7833–7835.

Rao MS, Sun Y, Escary JL, Perreau J, Tresser S, Patterson PH, Zigmond RE, Brulet P, Landis SC. 1993. Leukemia inhibitory factor mediates an injury response but not a target-directed developmental transmitter switch in sympathetic neurons. *Neuron 11*:1175–1185.

Robinson RC, Grey LM, Staunton D, Vankelecom H, Vernallis AB, Moreau JF, Stuart DI, Heath JK, Jones EY. 1994. The crystal structure and biological function of Leukemia Inhibitory Factor: Implications for receptor binding. *Cell 77*:1101–1116.

Robledo O, Auguste P, Coupey L, Praloran V, Chevalier S, Pouplard A, Gascan H. 1996. Binding interactions of leukemia inhibitory factor and ciliary neurotrophic factor with the different subunits of their high affinity receptors. *J Neurochem 66*:1391–1399.

Seto MH, Harkins RN, Adler M, Whitlow M, Church WB, Croze E. 1995. Homology model of human interferon-8 and its receptor complex. *Protein Sci 4*:655–670.

Simpson RJ, Hammacher A, Smith DK, Matthews JM, Ward LD. 1997. Interleukin-6: Structure–function relationships. *Protein Sci 6*:929–955.

Sippl MJ. 1993. Recognition of errors in three-dimensional structures of proteins. *Proteins Struct Funct Genet 17*:355–362.

Smith DK. 1996. Structural studies of leukaemia inhibitory factor (LIF) and its receptors [thesis]. Melbourne, Australia: University of Melbourne.

Smith DK, Treutlein HR, Maurer T, Owczarek CM, Layton MJ, Nicola NA, Norton RS. 1994. Homology modelling and ^{1}H NMR studies of human leukaemia inhibitory factor. *FEBS Lett 350*:275–280.

Somers W, Ultsch M, de Vos AM, Kossiakoff AA. 1994. The X-ray structure of a growth hormone–prolactin receptor complex. *Nature 372*:478–481.

Sprang SR, Bazan JF. 1993. Cytokine structural taxonomy and mechanisms of receptor engagement. *Curr Opin Struct Biol 3*:815–827.

Stewart CL, Kaspar P, Brunet LJ, Bhatt H, Gadi I, Köntgen F, Abbondanzo SJ. 1992. Blastocyst implantation depends on maternal expression of leukaemia inhibitory factor. *Nature 379*:76–79.

Sundström M, Lundqvist T, Rödin J, Giebel LB, Milligan D, Norstedt G. 1996. Crystal structure of an antagonist mutant of human growth hormone, G120R, in complex with its receptor at 2.9 resolution. *J Biol Chem 271*:32197–32203.

Tham S, Dowsing B, Finklestein D, Donato R, Surinda SS, Bartlett PF, Morrison WA. 1997. Leukemia inhibitory factor enhances the regeneration of transected rat sciatic nerve and the function of reinnervated muscle. *J Neurosci Res 47*:208–215.

Walter MR, Windsor WT, Nagabhushan TL, Lundell DJ, Lunn CA, Zauodny PJ, Narula SK. 1995. Crystal structure of a complex between interferon- and its soluble high-affinity receptor. *Nature 376*:230–235.

Ware CB, Horowitz MC, Renshaw BR, Hunt JS, Liggit D, Koblar SA, Gliniak BC, McKenna HJ, Papayannopoulou T, Thoma B, Cheng L, Donovan PJ, Peschon JJ, Bartlett PF, Willis CR, Wright BD, Carpenter MK, Davison BL, Gearing DP. 1995. Targeted disruption of the low-affinity leukemia inhibitory factor receptor gene causes placental, skeletal, neural and metabolic defects and results in perinatal death. *Development 121*:1283–1299.

Wells JA. 1996. Binding in the growth hormone receptor complex. *Proc Natl Acad Sci USA 93*:1–6.

Wells JA, de Vos AM. 1996. Hematopoietic receptor complexes. *Annu Rev Biochem 65*:609–634.

Woodcock JM, Bagley CJ, Zacharakis B, Lopez AF. 1996. A single tyrosine residue in the membrane-proximal domain of the granulocyte-macrophage colony-stimulating factor, interleukin (IL)-3, and IL-5 receptor common β-chain is necessary and sufficient for high affinity binding and signaling by all three ligands. *J Biol Chem 271*:25999–26006.

Yawata H, Yasukawa K, Shunji N, Murakami M, Yamasaki K, Hibi M, Taga T, Kishimoto T. 1993. Structure–function analysis of human IL-6 receptor: Dissociation of amino acid residues required for IL-6 binding and for IL-6 signal transduction through gp130. *EMBO J 12*:1705–1712.

Zhang JG, Owczarek CM, Ward LD, Howlett GJ, Fabri LJ, Roberts BA, Nicola NA. 1997. Evidence for the formation of a heterotrimeric complex of leukaemia inhibitory factor with its receptor subunits in solution. *Biochem J 325*:693–700.

Zurawski SM, Vega F, Doyle EL, Huyghe B, Flaherty K, Mckay DB, Zurawski G. 1993. Definition and spatial location of mouse interleukin-2 residues that interact with its heteromeric receptor. *EMBO J 12*:5113–5119.